FEATURE BASED HANDLING OF SURFACE FAULTS IN COMPACT DISC PLAYERS

Peter Fogh Odgaard [*,1] **Jakob Stoustrup** [*]
Palle Andersen [*] **Mladen Victor Wickerhauser** [**]
Henrik Fløe Mikkelsen [***]

[*] *Department of Control Engineering, Aalborg University, Fredrik Bajers Vej 7C, DK-9220 Aalborg East, Denmark*
[**] *Department of Mathematics, Campus Box 1146, Washington University, One Brookings Drive, St. Louis, MO 63130, USA*
[***] *Bang & Olufsen A/S, Peter Bangs Vej 15, DK-7600 Struer, Denmark*

Abstract: Compact Disc players have been on the market in more than two decades, and a majority of the involved control problems have been solved. However, there are still problems with playing Compact Discs related to surface faults like scratches and fingerprints. Two servo control loops are used to keep the Optical Pick-up Unit focused and radially on the information track of the Compact Disc. The problem is to design servo controllers which are well suited for handling surface faults which disturbs the position measurement and still react sufficiently against normal disturbances like mechanical shocks. In this paper a novel method called feature based control is presented. The method is based on a fault tolerant control scheme, which uses extracted features of the surface faults to remove those from the detector signals used for control during the occurrence of surface faults. The extracted features are Karhunen-Loève approximations of the surface faults. The performance of the feature based control scheme controlling Compact Disc Players playing Compact Discs with surface faults have been validated by experimental work with positive conclusive results.

Keywords: CD-Player, Fault Tolerant Control, Approximations, Fault Detection and Isolation

1. INTRODUCTION

Optical disc players such as Compact Disc players (CD-players) have in the past couple of decades been widely used in homes and businesses. However, performance issues are still to be improved on. A common problem with optical disc players is that they have problems playing certain discs with surface faults like scratches and fingerprints. An Optical Pick-up Unit (OPU) is used to retrieve the data/music stored in the information track on the disc. A main character of the CD-Player is the lack of physical contact between the OPU and the disc surface. Instead a servo loops are formed to keep the OPU focused at reflection layer of the disc. Another servo loop keep the OPU radially tracked on the spiral shaped data track.

[1] Corresponding author: Phone: +4596358744, Fax: +45 98151739, email: odgaard@control.aau.dk

The OPU includes optics which facilitate measures of the focus and radial distances, each calculated as the difference of signals from two photo detectors. The distances are the distance from the actual position of the OPU to the position where the OPU is focused and radially tracked. These focus and radial distances are also important in terms of detecting surface faults. The real problem with surface faults is that they degenerate the measures of focus and radial distances, whereas missing informations can be reconstructed due to redundancy in data.

One possible method to handle these faults is to use a fault tolerant control strategy, where the surface faults are handled in a special way, when detected. Faults are detected as fast as possible and when a fault is detected, the control strategy is changed in a way that accommodates the detected fault. A frequently used method for detection of faults is to observe changes in either the sum of focus signals or the sum of the radial signals, since a fault would reduce these sums, see (Philips, 1994), (Andersen *et al.*, 2001) and (Vidal *et al.*, 2001*b*). A simple fault tolerant control strategy is often used to handle such surface faults. The core idea is not to rely on sensor information during the fault. The sensor signals are simply fixed to zero as long as a fault is detected. In the sequel, we shall present an alternative to the use of the sum signals as residuals.

The research in control of CD-players has been intense in other directions than fault tolerant control, especially in adaptive and robust controllers applied to the CD-player. The first application of a μ-controller used in a CD-player was reported in (Steinbuch *et al.*, 1992), which was based on DK-iterations. An example of an adaptive control design was (Draijer *et al.*, 1992) where a self-tuning controller was suggested. Automatic adjustment of gain in dependence of the reflective characteristics is standard in commercial CD-players. A large number of different control strategies were applied to the CD-player. An adaptive repetitive method was suggested in (Dötch *et al.*, 1995), quantitative feedback theory was used in (Hearns and Grimble, 1999). In (Li and Tsao, 1999) rejection of non/repeatable disturbances was used, fuzzy control was used by (Yen *et al.*, 1992). In (Yao *et al.*, 2001) a hybrid fuzzy control was designed, linear quadratic Gaussian control was used in (Weerasooriya and Phan, 1995) and a disturbance observer was designed in (Fujiyama *et al.*, 1998). A vibration absorber to damp the mechanical disturbances was used in (Wook Heo and Chung, 2002). Only (Vidal Sánchez, 2003) addresses the use of FTC in the handling of surface faults such as scratches, fingerprints etc. The surface faults impose an upper limit on the controller bandwidth, which is in conflict with the minimization of the disturbances channels, since those controllers have a high bandwidth. (Heertjes and Sperling, 2003) and (Heertjes and Steinbuch, 2004) indirectly handle the surface faults by the use of non-linear filters to improve controller sensibility without making the controllers more sensitive towards the surface faults.

In this paper a control scheme based on fault tolerant control and signal processing is presented. This scheme has been studied in the Ph.D work by the first author, see (Odgaard, 2004). This scheme is called feature based control, since features are extracted from the surface faults and subsequently used to remove the influence from surface faults on the distance signals. The standard nominal controllers can subsequently be used to control the focusing and radial tracking. This feature based control scheme uses some previous published results: estimation of more discriminating residuals and distance signals during a surface fault see (Odgaard *et al.*, 2003*a*), time localization and fault detection of surface faults see (Odgaard and Wickerhauser, 2003*b*), fault classification of surface faults see (Odgaard and Wickerhauser, 2003*a*), and a simulation model of CD-players playing CDs with surface faults (Odgaard *et al.*, 2003*d*).

A short description of focus and radial servos in the CD-player is given together with a description of the relevant model. The general structure of the feature based control scheme is presented, followed by the major contribution of this paper, which is the fault accommodation part of the feature based control scheme. It is proven that this scheme is stable given the linear model of the CD-player. Finally the performance of the control scheme is validated by experimental work, where clear improvements in the handling of the surface faults are seen.

2. DESCRIPTION AND MODEL OF THE COMPACT DISC PLAYER

The OPU in the CD-player is focused and radially tracked by movements of the OPU in two directions, called focus and radial directions. These movements are enabled by a two axis device, where linear electro-magnetic actuators are used to perform the actual movements. The positions of the OPU in the two directions are measured by using smart optics in the OPU. The OPU generates four detector signals which can be used to generate the approximations of the distances. The two focus detector signals, D_1 and D_2 are formed by the use of the single Foucault principle illustrated in Fig. 1, which is applied to the main laser beam. The upper part illustrates the

situation where the OPU is focused, $D_1 - D_2 = 0$. Followed by the situation where the OPU is too close to the disc, $D_1 - D_2 > 0$, and the situation where the OPU is too far away from the disc, $D_1 - D_2 > 0$. The radial detector signals are formed by

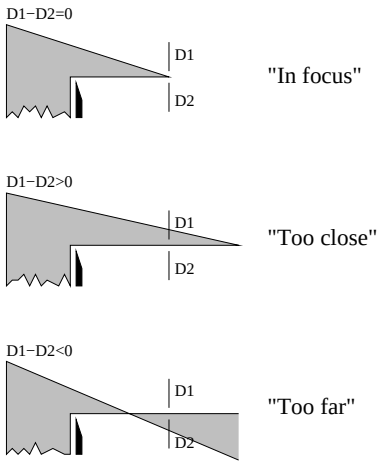

Fig. 1. Illustration of the single foucault focus detector principle.

the use of two additional side beam place relative to the main beam with an offset a_k as illustrated in Fig. 2. Each of the side beams are detected by a separate detector, S_1 and S_2. The energies in the reflected beams depend on their respective placement over the track. I.e. if the main spot is centered over the track, $S_1 - S_2 = 0$, else if the main spot is to the right, $S_1 - S_2 < 0$, and if it is to much to the left $S_1 - S_2 > 0$.

Unfortunately these measurements are influenced by surface faults. All this is illustrated by Fig. 3. In this figure the signals are defined as follows. $\mathbf{u}[n]$ is a vector of the control signals to the electro-magnetic system, $\mathbf{d}[n]$ is a vector of the unknown disturbances to the electro-magnetic system, $\mathbf{d}_\mathrm{ref}[n]$ is vector of the unknown references to the system, $\mathbf{e}[n]$ is a vector of the focus distances, $\mathbf{s}_\mathrm{m}[n]$ is the measured detector signals, $\mathbf{s}[n]$ is detector signals without surface faults and $\mathbf{s}_\mathrm{m}[n]$ is vector of the measured detector signals.

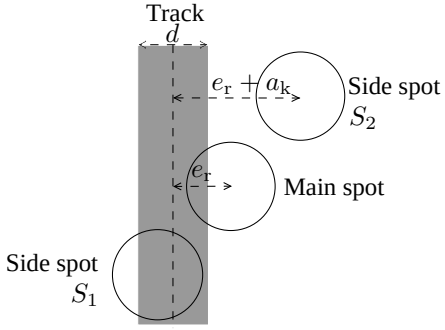

Fig. 2. Illustration on how the three beams are placed relative to each other on the disc surface.

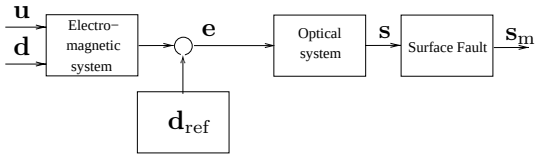

Fig. 3. The principles of the model of the CD-player. The CD-player consists of four parts. The electro-magnetic system and the optical system, the unknown references (in a vector denoted $\mathbf{d}_\mathrm{ref}[n]$) and the surface fault. $\mathbf{u}[n]$ is a vector of the control signals to the electro-magnetic system, $\mathbf{d}[n]$ is a vector the unknown disturbances to the electro-magnetic system, $\mathbf{e}[n]$ is a vector of the distances, $e_\mathrm{r}[n]$ is the radial distance, $\mathbf{s}[n]$ is vector of the detector signals without surface faults and $\mathbf{s}_\mathrm{m}[n]$ is vector of the measured detector signals.

2.1 Model of the electro-magnetic system

The electro-magnetic system in the CD-player is modeled and described in a number of publications. The focus and radial model are much alike, and are often modeled by decoupled second order models, see (Stan, 1998), (Vidal *et al.*, 2001*a*), (Bouwhuis *et al.*, 1985) and (Vidal *et al.*, 2001*b*).

$$\dot{\eta}(t) = \mathbf{A} \cdot \eta(t) + \mathbf{B} \cdot \mathbf{u}(t), \tag{1}$$

$$\begin{bmatrix} e_\mathrm{f}(t) \\ e_\mathrm{r}(t) \end{bmatrix} = \mathbf{C} \cdot \eta(t), \tag{2}$$

where

$$\mathbf{A} = \begin{bmatrix} \mathbf{A}_\mathrm{f} & \mathbf{0} \\ \mathbf{0} & \mathbf{A}_\mathrm{r} \end{bmatrix} \in \mathcal{R}^{4\times 4}, \tag{3}$$

$$\mathbf{B} = \begin{bmatrix} \mathbf{B}_\mathrm{f} & \mathbf{0} \\ \mathbf{0} & \mathbf{B}_\mathrm{r} \end{bmatrix} \in \mathcal{R}^{4\times 2}, \tag{4}$$

$$\mathbf{C} = \begin{bmatrix} \mathbf{C}_\mathrm{f} & \mathbf{0} \\ \mathbf{0} & \mathbf{C}_\mathrm{r} \end{bmatrix} \in \mathcal{R}^{2\times 4}, \tag{5}$$

where $\eta(t)$ is the vector of states in the model, $\mathbf{A}_\mathrm{f}, \mathbf{B}_\mathrm{f}, \mathbf{C}_\mathrm{f}$ are the model matrices in the focus model, and $\mathbf{A}_\mathrm{r}, \mathbf{B}_\mathrm{r}, \mathbf{C}_\mathrm{r}$ are the model matrices in the radial model. This model is somewhat simplified, but sufficient for our purposes.

2.2 Model of the optical detectors

This optical model is expressed by the vector mapping, described in (6).

$$\mathbf{f}: \quad \left(\begin{bmatrix} e_\mathrm{f}(t) \\ e_\mathrm{r}(t) \end{bmatrix} \right) \rightarrow \begin{bmatrix} D_1(t) \\ D_2(t) \\ S_1(t) \\ S_2(t) \end{bmatrix}, \tag{6}$$

where $D_1(t)$ and $D_2(t)$ are the two focus detectors and $S_1(t)$ and $S_2(t)$ are the two radial detectors.

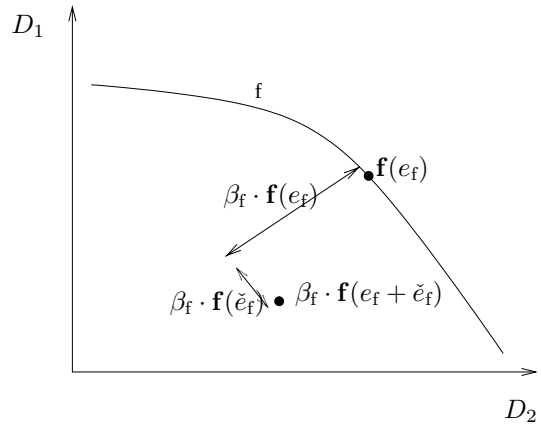

Fig. 4. Illustration of how the surface fault influence the focus measurements D_1 and D_2. $\beta \cdot \mathbf{f}(\mathbf{e} + \check{\mathbf{e}})$ is the measured point parameterized with β and $\check{\mathbf{e}}$. $\mathbf{f}(\mathbf{e})$ is point where the measurements would have been if no surface have been present.

These mappings can be simplified using the following simplification, see (Odgaard *et al.*, 2003*c*).

$$f_i(e_\mathrm{f}(t), e_\mathrm{r}(t)) \approx h_i(e_\mathrm{f}(t)) \cdot g_i(e_\mathrm{r}(t)), \quad (7)$$

where

$$i \in \{1, 2, 3, 4\}, \quad (8)$$

moreover

$$g_1(e_\mathrm{r}(t)) = g_2(e_\mathrm{r}(t)). \quad (9)$$

In (Odgaard *et al.*, 2003*c*), detailed optical models are described. In practise it is useful to simplify this model, in (Odgaard *et al.*, 2003*c*) and (Odgaard *et al.*, 2004) it is suggested to approximate $h_i(e_\mathrm{f}[n])$ and $g_i(e_\mathrm{r}[n])$ with cubic splines.

2.3 Model of the surface faults

The surface faults decreases the energy received in all the detectors. This can be described by scaling the photo detector signals, such that the two focus detectors are scaled with one scale, $\beta_\mathrm{f}(t)$, and the two radial detectors are scaled with another one, $\beta_\mathrm{r}(t)$. However if these scalings were the only influence from the surface faults on the detector signals, the surface fault components could be removed from the detector signals by normalization of the detector signals. The surface fault introduces a pair of faulty distance components represented by a vector $\check{\mathbf{e}}(t)$, see (Odgaard *et al.*, 2003*b*) and (Odgaard *et al.*, 2003*d*). These surface faults components are illustrated for the focus detector in Fig. 4.

This leads to the following model of the detector signals during a surface fault.

$$\mathbf{s}_\mathrm{m}(t) = \begin{bmatrix} \beta_\mathrm{f}(t) \cdot \mathbf{I} & \mathbf{0} \\ \mathbf{0} & \beta_\mathrm{r}(t) \cdot \mathbf{I} \end{bmatrix} \cdot \mathbf{f}\left(\mathbf{e}(t) + \check{\mathbf{e}}(t)\right). \quad (10)$$

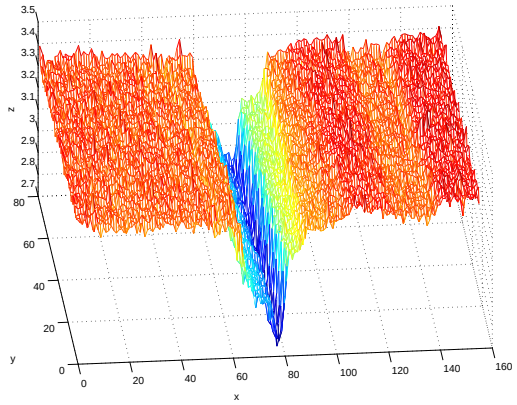

Fig. 5. 3-D plot of $\beta_\mathrm{f}[n]$ in sequential fault encounters. The duration and depth of the fault increases. The x-axis is samples of yth encounter, (the y-axis is the encounter number), and the z-axis is $\beta_\mathrm{f}[n]$. Notice the small variations from encounter to encounter.

An important remark is that a surface fault does not vary much from one encounter to the next encounter. This is illustrated in Fig. 5, where $\beta_\mathrm{f}[n]$ of a small scratch from 78 revolutions is illustrated.

2.4 Experimental setup and practical considerations

The experimental setup consists of a CD-player, with a three beam single Foucault detector principle, a PC with an I/O-card, and some hardware in order to connect the CD-player with the I/O-card. Due to the limited computational power of the CPU in the PC the sample frequency is chosen to 35 kHz. This is lower than the normal CD-servo sample frequency (44 kHz). The four detector signals and the two control signals are sampled. It is possible to control focus and radial distance by the use of PC or by using the built-in controller of the CD-player.

In the following the system is viewed as a discrete time system meaning that the models used are discretized with the samplings frequency of 35 kHz. This means that defined model is discretized as well.

3. FEATURE BASED CONTROL OF COMPACT DISC PLAYERS

In this section the core of the feature based control scheme of the CD-player will be described and designed. The idea in short is, that the residuals are used to detect and locate the surface faults. The feature extraction presented in (Odgaard and Wickerhauser, 2003*a*) gives a classification of the fault. Approximating coefficients of the surface faults in a given basis representing the class of the

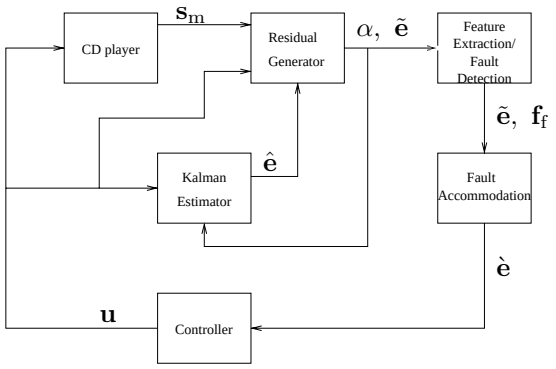

Fig. 6. Illustration of the structure of the feature based control scheme, to handle surface faults as faults. $\mathbf{s}_\mathrm{m}$ is vector of the measured detector signals, α is a vector of the residuals, $\tilde{\mathbf{e}}$ is a vector of the static estimates of the distances, $\mathbf{f}_\mathrm{f}$ is a vector the fault features, $\hat{\mathbf{e}}$ is a vector of the dynamical estimates of the distances, $\grave{\mathbf{e}}$ is a vector of the corrected distances, $\mathbf{u}$ is a vector of the control signals.

fault has been presented in (Odgaard *et al.*, 2002) and (Odgaard *et al.*, 2003*d*). This approximation of the surface faults is used to remove the fault component from the measurement of the next surface fault encounter. Since the fault component is removed from the detector signals standard focus and radial controllers can be used.

The feature based control strategy is illustrated in Fig. 6, from which it can be seen that the feature based control strategy consists of: residual generator, Kalman estimator, feature extraction/fault detection and fault accommodation. The residual and distance estimation estimate a pair of decoupled residuals and focus and radial distances. These decoupled residuals are defined as:

$$\begin{bmatrix}\alpha_\mathrm{f}[n]\\ \alpha_\mathrm{r}[n]\end{bmatrix} = \begin{bmatrix}1-\beta_\mathrm{f}[n]\\ 1-\beta_\mathrm{r}[n]\end{bmatrix} \tag{11}$$

The residual generator provides a pair of alternative residuals and a static estimate of focus and radial distance based on detector signals. The Kalman estimator is applied to these static estimates in order to compute more reliable focus and radial distances.are described in details in (Odgaard *et al.*, 2003*a*). The Kalman estimator is also used to estimate the distance signals during surface faults. It is optional to use the alternative residuals to detect the surface faults, the normally used sum signals can be used instead.

The fault detection detects and locates the fault in time. The time localization gives information of when to extract features and when to accommodate the fault. It can be done by the use of simple thresholds or by the methods presented in (Odgaard and Wickerhauser, 2003*b*), where time-frequency based methods are used to design filters for detections of the faults. However, the conclusion in (Odgaard and Wickerhauser, 2003*b*) is it is preferable to adapt a thresholding algorithm to problems encountered in the detection of the surface faults.

The feature extraction provides the fault accommodation with the class of the fault, see (Odgaard and Wickerhauser, 2003*a*), and approximating coefficients in the Karhunen-Loève basis of the given class of the fault, see below.

The fault accommodation is performed by removing the surface fault component from the measured distance signals by subtracting the fault approximation.

From these it can be seen that the feature based control strategy is strongly related to a fault tolerant control scheme. The fault detection/locator performs the fault detection, by locating the fault in time. In this application only surface faults are considered, so fault isolation is not required. The estimation of the fault is performed by fault classification and approximation of the fault, where a disturbance decoupled fault estimation is performed. This means that the fault detection together with the feature extraction form the fault diagnosis. These parts provide the fault accommodation with the information needed for handling the surface faults.

In (Odgaard *et al.*, 2003*d*), the surface faults were simulated by the use of Karhunen-Loève approximations. It is seen that just a few Karhunen-Loève basis vectors can be used to approximate the surface faults very well, see Fig. 7, where approximations with one and four basis vectors are compared to surface faults extracted from measurements. The idea is now to subtract that approximations from the measured detector signals the next time the fault is encountered before the measurements are fed to the nominal controllers. The algorithm will be described in the following section.

4. FAULT ACCOMMODATION BY REMOVAL OF THE SURFACE FAULT

It has previously been stated that a fault does not vary much from one encounter to the next encounter. This means that an approximation of the fault at encounter ϑ can be subtracted from the fault at encounter $\zeta + 1$. This will almost remove the fault from the measured signals as well as it could if the approximation was used at encounter ζ. The signals used in the following are defined as follows: $\mathbf{e}[n]$ is a vector of focus and radial distances, $\check{\mathbf{e}}[n]$ is a vector of faulty sensor components due to the surface fault, $\tilde{\check{\mathbf{e}}}[n]$ is a vector of the estimates of the faulty sensor components due to the surface fault. $\mathbf{e}_\mathrm{m}[n]$ is a vector of the measured distance signals and $\mathbf{n}_\mathrm{m}[n]$ is a vector of the measurement noises. The

relations among these signals are illustrated in Fig. 8.

4.1 Karhunen-Loève approximations

Given a matrix, $\mathbf{X}$, of u column vectors in $\mathcal{R}^m$, where $u > m$, the Karhunen-Loève basis minimizes the average linear approximation error of the vectors in the set, (Mallat, 1999). Another advantage of the Karhunen-Loève basis is that it approximates the general structures of all the signals in $\mathbf{X}$ with just a few basis vectors, meaning it can be used to compress the signals in $\mathbf{X}$, see (Mallat, 1999) and (Wickerhauser, 1994*b*) and (Saito, 1998). The Karhunen-Loève basis has been used to a compression problem of pictures of faces, in (Wickerhauser, 1994*a*). This data set of pictures of faces (128×128 pixels, eight bit gray scale with several thousand faces, see (Wickerhauser, 1994*a*)) constitutes a very large data set. The idea was to extract certain features from these pictures of faces, in order to identify one face among all the others. Dealing with feature extraction from a large size data set is problematic. Size of the data set was as a consequence reduced by the use of the Karhunen-Loève basis, (Wickerhauser, 1994*a*), without removing the general structures of the data, since these general structures are remaining. The important features can still be extracted from the data set, It is whereby still possible to identify a given face from the data set, see (Wickerhauser, 1994*a*). In (Kraut *et al.*, 2004) another usage of the Karhunen-Loève basis was reported, where it was used for efficient estimations of tropospheric refractivity using radar clutter.

The Karhunen-Loève basis is computed based on $\mathbf{X}$, first of all it is assumed that the column vectors in $\mathbf{X}$ has zero mean, if not a preliminary step is introduced in order to fulfill that assumption. The Karhunen-Loève basis, $\mathcal{K}$, can be defined as

$$\mathcal{K} = \{v_1, \cdots, v_m\}, \tag{12}$$

is an orthornomal basis of eigenvectors of the matrix $\mathbf{X}\mathbf{X}^T$, ordered in such a way that v_n is associated with the eigenvector λ_n, and $\lambda_i \geq \lambda_j$ for $i > j$. A matrix of the basis vectors can following be defined as

$$\mathbf{K}_{\mathrm{L}} = \left[v_m, v_{m-1}, \cdots, v_i\right] \tag{13}$$

So in other words the Karhunen-Loève basis is the eigenvectors of the autocorrelation of $\mathbf{X}$. The eigenvalues of the autocorrelation have the values of the variances of the related Karhunen-Loève basis vectors. The approximating properties of the Karhunen-Loève basis vectors are sorted in increasing order, that means that if the basis consists of p vectors the basis vector p is the most approximating basis vector. In addition the

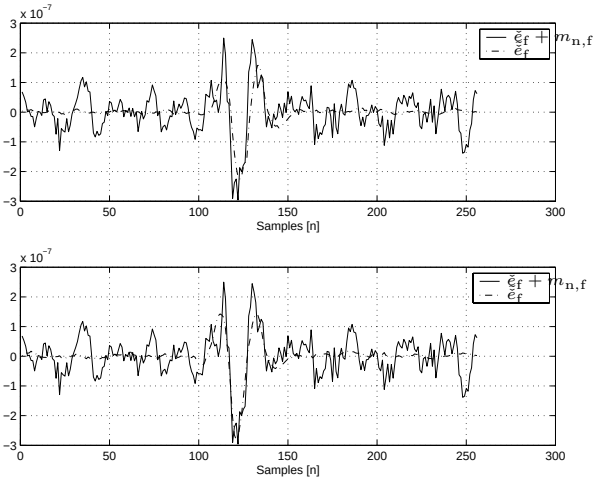

Fig. 7. Illustration of the Karhunen-Loève approximation of $\check{e}_{\mathrm{f}} + m_{\mathrm{n,f}}$ which contains a typical scratch. The approximation is denoted with $\tilde{\check{e}}_{\mathrm{f}}$. The first approximation is based on the most approximating coefficient, the second approximation is based on the four most approximating coefficients.

general structures in all the vectors in $\mathbf{X}$ are represented by only a few basis vectors. The remaining basis vectors represent the signal parts which are not general for $\mathbf{X}$, i.e. noises in the signal, etc.

As a consequence of these excellent approximating qualities of the Karhunen-Loève basis, $\mathcal{K}$, has been chosen to approximate the fault by using the q most approximating Karhunen-Loève basis vectors, $\mathbf{K}_{\check{e}}$. Consequently the remaining basis vectors, $\mathbf{K}_{\mathrm{n}}$, span the noises and disturbances in the distances signals. In Fig. 7 the approximation of the scratch by the four most approximating Karhunen-Loève basis vector is illustrated.

$$\mathbf{K}_{\mathrm{L}} = \left[\mathbf{K}_{\mathrm{n}}\ \mathbf{K}_{\check{e}}\right], \tag{14}$$

where

$$\mathbf{K}_{\mathrm{L}} \in \mathcal{R}^{(m\times m)}, \tag{15}$$

$$\mathbf{K}_{\mathrm{n}} \in \mathcal{R}^{(m\times(m-q))}, \tag{16}$$

$$\mathbf{K}_{\check{e}} \in \mathcal{R}^{(m\times q)}, \tag{17}$$

$$q \ll m. \tag{18}$$

Based on (14) the fault component in the measured distance signals can be separated from the measurement noises, which $\mathbf{K}_{\check{\mathbf{e}}}$ is constructed not to support. In addition an observation has been made by inspection of the measured data, that the disturbances give small projections on $\mathbf{K}_{\check{\mathbf{e}}}$. The reconstruction of measured signals without this surface will reduce the fault component of focus and radial distances dramatically.

An estimate of $\check{\mathbf{e}}[n]$ during a fault at encounter ϑ can be computed by

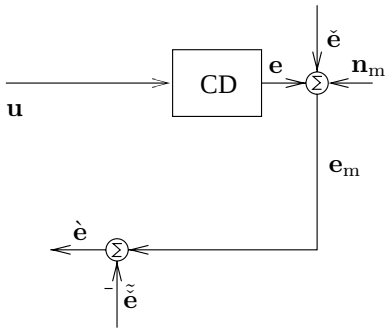

Fig. 8. Illustration of the signals used in the feature based control scheme. CD is the OPU and electro-magnetic actuators in the CD-player. $\mathbf{u}$ is a vector of the control signals, $\mathbf{e}$ is a vector of focus and radial distances, $\check{\mathbf{e}}$ is a vector of faulty sensor components due to the surface fault, $\tilde{\check{\mathbf{e}}}$ is a vector of the estimates of the faulty sensor components due to the surface fault. $\mathbf{e}_{\mathrm{m}}$ is a vector of the measured distance signals and $\mathbf{n}_{\mathrm{m}}$ is a vector of the measurement noises.

$$\tilde{\check{\mathbf{e}}} = \begin{bmatrix} \mathbf{K}_{\check{e}_{\mathrm{f}}} \mathbf{K}_{\check{e}_{\mathrm{f}}}^T \cdot \left(e_{\mathrm{m,f}}^L[\vartheta] - \hat{e}_{\mathrm{f}}^L[\vartheta] \right) \\ \mathbf{K}_{\check{e}_{\mathrm{r}}} \mathbf{K}_{\check{e}_{\mathrm{r}}}^T \cdot \left(e_{\mathrm{m,r}}^L[\vartheta] - \hat{e}_{\mathrm{r}}^L[\vartheta] \right) \end{bmatrix}. \tag{19}$$

Here $\cdot^L[\vartheta]$ denotes the lifted signals, where the ϑth fault encounter begins at sample no. n_ϑ.

In the following a recurrent system is defined as a system where specific signal sequences of constant window lengths are recurring with none specific intervals. The length of these signals sequences are denoted l_w and the windows begins at samples $T_1, T_2 \cdots$.

A more detailed description of the lifting operator is given in (Wisniewski and Stoustrup, 2001) and (Khargonekar *et al.*, 1985). The lifting operator L is an isometric isomorphism which transforms a linear recurrent system to a time invariant representation defined as following

$$L : (y_0, y_1, \cdots)^T \mapsto \begin{bmatrix} (y_{T_1}, y_{T_1+1}, \cdots, y_{T_1+l_w-1}, \cdots) \\ (y_{T_2}, y_{T_2+1}, \ldots, y_{T_2+l_w-1}) \\ \vdots \end{bmatrix}^T, \tag{20}$$

where y is the signal which shall be lifted. In this case, the window length is equal m, since it is the length of the Karhunen-Loève basis vectors.

In order to use the approximation in (19), it is needed to estimate $\hat{\mathbf{e}}[n]$ by the use of a Kalman estimator described in (Odgaard *et al.*, 2003*a*). However, if $\hat{\mathbf{e}}[n]$ do not have large projections of $\mathbf{K}_{\check{\mathbf{e}}}$, (19) can be approximated by (21).

$$\tilde{\check{\mathbf{e}}} = \begin{bmatrix} \mathbf{K}_{\check{e}_{\mathrm{f}}} \mathbf{K}_{\check{e}_{\mathrm{f}}}^T \cdot e_{\mathrm{m,f}}^L[\vartheta] \\ \mathbf{K}_{\check{e}_{\mathrm{r}}} \mathbf{K}_{\check{e}_{\mathrm{r}}}^T \cdot e_{\mathrm{m,r}}^L[\vartheta] \end{bmatrix}. \tag{21}$$

The Kalman estimator is only used to estimate $\hat{\mathbf{e}}[n]$, this means that a consequence of (21) is that the Kalman estimator is not needed in the closed loop feature based control scheme, but it is needed in order to compute the Karhunen-Loève basis of the surface faults. This means that if focus and radial distances are in the nominal operation range, the faults can be approximated by the use of the normalized focus and radial difference signals:

$$e_{\mathrm{m,f}}[n] \approx k_{\mathrm{f}} \cdot \frac{D_1[n] - D_2[n]}{D_1[n] + D_2[n]}, \tag{22}$$

$$e_{\mathrm{m,r}}[n] \approx k_{\mathrm{r}} \cdot \frac{S_1[n] - S_2[n]}{S_1[n] + S_2[n]}, \tag{23}$$

where k_{f} is the optical gain in the focus loop and k_{r} is the optical gain in the radial loop.

Due to limitations in the PC computational powers only the approach with out the Kalman estimator is tested on the test setup. An extension of the proposed method could contain an adaptive scheme where the basis is trained based on faults on a given CD.

The stability and performance issue of the removal is dealt with in Section 5.

The approximation of the surface fault is now computed. The next problem is to determine when to begin the correction of focus and radial distances. This involves a synchronization of the correction with the distance signals, where a correct synchronization results in a removal of the fault from the measurements. An incorrect synchronization might result in an increase of the controller reaction to the surface fault, and could actually make the problem with the surface faults more severe than if no correction was performed.

4.2 Synchronization of the fault removal

In order to synchronize the correction of the measured signals two methods were used: detection of beginning and end of the surface fault, and prediction of the next fault based on previous encounters of the faults. The first method uses detection at a given fault to correct this given fault. This method has a good synchronization, but unfortunately has the drawback that it locates the beginning and end of the faults respectively too late and too early. Using the previous location of the fault in time to predict the next fault, makes it possible to begin and end the correction at a more correct time than if detection based on the given fault is used. This prediction is based on some time localization scheme e.g. the one developed in (Odgaard and Wickerhauser, 2003*b*). However, it is not possible in practical settings to predict the placement of a fault. The reason for this is the implementation of the controller of the disc motor, which should guarantee a constant linear speed of the OPU relative to the track. However, this controller is implemented in a way that does not result in a constant linear speed but only in a linear speed in intervals.

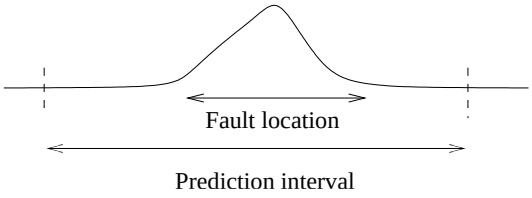

Fig. 9. Illustration on the fault location and the interval in which the fault is located.

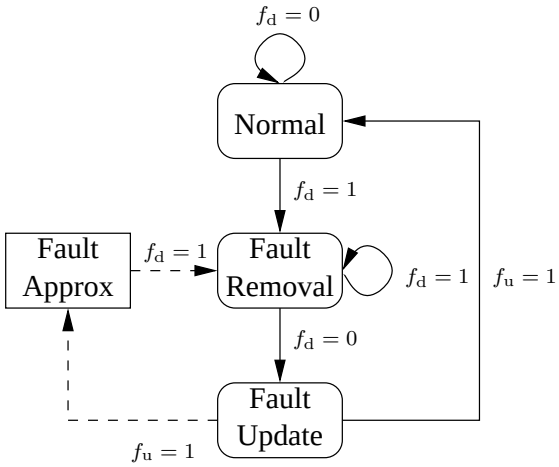

Fig. 10. Illustration of the feature based control scheme illustrated as a state machine. The dashed lines do not illustrate state changes but data transfers. f_d denotes the detection signal, if a fault is detected at sample n it has 1 as its value, if a fault is not present it takes the value 0. f_u denotes an indication of the fault has been updated. The Fault Removal represents step 2 in the feature based control scheme and Fault Update represents step 3-5 in this scheme.

In practice a combination of the two fault localization methods are used. The prediction, based on the time localization methods presented in (Odgaard and Wickerhauser, 2003*b*), is used to give an interval in which the fault is located and in this interval a lower threshold, than if the prediction was not used, can be used, see Fig. 9.

4.3 The algorithm of the feature based control strategy

The fault correction algorithm can now be stated:

(1) Detect the fault and locate its position in time, when the fault is detected at sample n, $f_\mathrm{d}[n] = 1$.
(2) If $f_\mathrm{d}[n] = 1$:

$$a = \begin{cases} 0 & \text{if } f_\mathrm{d}[n-1] = 0, \\ a+1 & \text{if } f_\mathrm{d}[n-1] = 1. \end{cases},$$

$$\grave{\mathbf{e}}[n] = \mathbf{e}_\mathrm{m}[n] - \begin{bmatrix} \tilde{\check{\mathbf{e}}}_\mathrm{f}[\iota] \\ \tilde{\check{\mathbf{e}}}_\mathrm{r}[\iota] \end{bmatrix},$$

where

$$\iota = ((256 - l_\mathrm{f}) \ \mathrm{div} \ (2)) + a,$$

where a is a counter counting the number of samples the given fault is present, and ι is a counter used to locate the given sample relative to the fault correction block.
(3) When the fault has been passed, classify the fault, time locate the fault, and compute the fault length l_f.
(4) Compute the focus correction block coefficients by: $\mathbf{k}_\mathrm{f} = \mathbf{K}_{\check{e}_\mathrm{f}} \cdot e_{\mathrm{m,f}}[\upsilon]$ and the radial correction coefficients by : $\mathbf{k}_\mathrm{r} = \mathbf{K}_{\check{e}_\mathrm{r}} \cdot e_{\mathrm{m,r}}[\upsilon]$, where υ is the interval of 256 samples in which the fault is present.
(5) Compute the focus fault removal correction block by: $\tilde{\check{\mathbf{e}}}_\mathrm{f} = \mathbf{K}_{\check{e}_\mathrm{f}} \cdot \mathbf{k}_\mathrm{f}$, and the radial fault removal correction by: $\tilde{\check{\mathbf{e}}}_\mathrm{r} = \mathbf{K}_{\check{e}_\mathrm{r}} \cdot \mathbf{k}_\mathrm{r}$.

In the following, $\mathcal{P}(\cdot)$ denotes an operator that maps measured signals into their fault components by applying the correction algorithm. Due to the design of $\mathbf{K}_{\check{\mathbf{e}}}$ it does in principle not make any difference if $\mathbf{e}_\mathrm{m}[n]$ or $\mathbf{e}_\mathrm{m}[n] - \hat{\mathbf{e}}[n]$ is used to estimate the surface fault, since $\mathbf{K}_{\check{\mathbf{e}}}$ is designed to support $\check{\mathbf{e}}[n]$ and assumed not support $\mathbf{e}_\mathrm{m}[n]$. This means that

$$\mathcal{P}\left(\mathbf{e}_\mathrm{m}\right)[n] \approx \mathcal{P}\left(\check{\mathbf{e}}\right)[n] \Rightarrow \quad (24)$$

$$\mathcal{P}\left(\hat{\mathbf{e}}\right)[n] \approx 0. \quad (25)$$

Which in turn implies that it is not necessary to estimate $\hat{\mathbf{e}}[n]$. The normed focus and radial differences, (22, 23), can be used instead and thereby saves computing power. Only the last version of the algorithm is implemented due to limitations in the computer power in the experimental setup.

4.4 Practical implementation of the algorithm

The implementation uses only the four most approximating basis vectors, of a given fault class for each of two distance signals. The four basis vectors are chosen in order to limit the number of computations in the algorithm, and since experiments have shown that these four basis vectors approximate the faults very well see above. In order to avoid book keeping algorithms it is assumed that the CD only has one scratch. The applied controllers are the frequently used PID-controllers see (Stan, 1998).

5. STABILITY AND PERFORMANCE OF THE FEATURE BASED CONTROL SCHEME

The feature based control strategy is illustrated in Fig. 11. This figure illustrates how the influence from the surface fault is removed by the use of $\mathcal{P}(\cdot)$. This means that the controller, K, reacts on the sum of $\mathbf{e}[n]$ and the measurement noises, n_m.

In the following some stability and performance issues of the algorithm will be discussed starting with dealing with the stability.

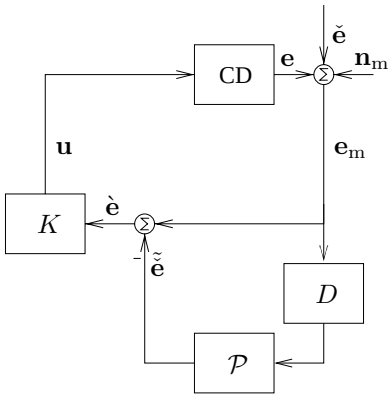

Fig. 11. Illustration of the closed loop with the feature based correction $\mathcal{P}$, K is the controller, and CD is the CD-player. Δ is the one revolution delay. $\mathbf{u}$ is a vector of the control signals, $\mathbf{e}$ is a vector of focus and radial distances, $\check{\mathbf{e}}$ is a vector of faulty sensor components due to the surface fault, $\tilde{\check{\mathbf{e}}}$ is a vector of the estimates of the faulty sensor components due to the surface fault. $\mathbf{e}_{\mathrm{m}}$ is a vector of the measured distance signals and $\mathbf{n}_{\mathrm{m}}$ is a vector of the measurement noises.

5.1 Stability

It is assumed that: K and CD are internally stable, and the nominal controller K stabilizes the plant CD, if $\check{e}[n]$ is zero or near zero. However, if $\check{\mathbf{e}}[n]$ increases it might force the CD-player outside its linear region and could cause an unstable closed loop. On the other hand if $\mathbf{e}[n] \approx \hat{\mathbf{e}}[n]$ the effect from the surface fault has been removed from the closed loop. This means that the control signal would be same as in the fault free case, meaning that the system is stable since it is nominally stable. $\mathcal{P}$ reconstruct the recurrent part of the measurement signals meaning that

$$\mathbf{e}_{\mathrm{m}} - \mathcal{P}\left(\mathbf{e}_{\mathrm{m}}\right) \approx= \mathbf{e} + \mathbf{n}_{\mathrm{m}}. \tag{26}$$

This can be achieved if

$$\check{\mathbf{e}} \approx \mathcal{P}\left(\mathbf{e}_{\mathrm{m}}\right) \Rightarrow \tag{27}$$

$$\mathcal{P}\left(\mathbf{n}_{\mathrm{m}}\right) \approx 0 \ \wedge \ \mathcal{P}\left(\mathbf{e}\right) \approx 0 \ \wedge \tag{28}$$

$$\check{\mathbf{e}} = \mathcal{P}\left(\check{\mathbf{e}}\right). \tag{29}$$

This is fulfilled if the approximating bases in $\mathcal{P}\left(\cdot\right)$ does approximate $\check{\mathbf{e}}[n]$ well and not $\mathbf{e}[n]$, $\mathbf{n}_{\mathrm{m}}[n]$. $\mathcal{P}\left(\cdot\right)$ is designed to be the best approximating basis of $\check{\mathbf{e}}[n]$. The Karhunen-Loève basis is not designed to support $\mathbf{e}[n]$, but no guarantees are given that it does not support $\mathbf{e}[n]$. Instead $\mathcal{P}\left(\cdot\right)$ might amplify the system dynamic in a degree that causes the entire system to be non-stable. From this it is clear that $\mathcal{P}\left(\cdot\right)$'s amplification of the system dynamic must be small, such that the energy in a given system response is decreased through $\mathcal{P}\left(\cdot\right)$ from revolution to revolution. By inspecting Fig. 11 the way the feature based control scheme influences the control loop, it can be observed that the influence can be analyzed by using the complementary sensitivity of the servo system. The influence from the feature based

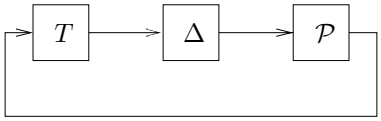

Fig. 12. Closed loop of the feature based control system. T is the complementary sensitivity of the nominal system, Δ is the one revolution delay, and $\mathcal{P}$ is the feature based fault handling.

fault handling on the nominal servo system can be inspected if the T denotes the complementary sensitivity of the nominal servo system, and Δ is the one revolution delay, see Fig. 12.

In order to combine these part systems, the complementary sensitivity of the nominal servo system and $\mathcal{P}$ are lifted, meaning that both part systems are represented by a discrete time series of a given length.

The lifted $\mathcal{P}$ can be computed by

$$\mathcal{P}^{\mathrm{L}} = \mathbf{K}_{\check{e}} \cdot \mathbf{K}_{\check{e}}^{T}, \tag{30}$$

and the lifted representation of the complementary sensitivity is

$$T^{\mathrm{L}} = \begin{bmatrix} h_0 & 0 & \cdots & 0 \\ h_1 & h_0 & & \vdots \\ \vdots & & \ddots & \\ h_{255} & \cdots & & h_0 \end{bmatrix}, \tag{31}$$

where $\mathbf{h} = [h_0 \ h_1 \ \cdots \ h_{255}]$ is time series of 256 samples of the impulse response of T.

By lifting the system illustrated in Fig. 12 one gets a set of discrete difference equations of the form, if :

$$\xi[N+1] = \mathbf{A}\xi[N] + \mathbf{K}\mathbf{u}[N], \tag{32}$$

where $\mathbf{A} = T^{\mathrm{L}}\mathcal{P}^{\mathrm{L}}$. These definitions make it possible to state Lemma 1, which says that the linear system is stable.

1 Lemma
The feature based control system defined by Fig. 11 is stable if and only if: max $\left(|eig\left(T^{L}\mathcal{P}^{L}\right)|\right) < 1$, *where* $\mathcal{P}^{L}$ *is defined in (30) and* T^{L} *is defined in (31).*

1 Proof of Lemma
Necessary and sufficient conditions:
The stability of the closed loop system shown in Fig. 11 is equiviliant to stability of the system in (32), which is a standard LTI discrete time system, from which the result follows, the system is stable if and only if max $\left(|eig\left(T^{L}\mathcal{P}^{L}\right)|\right) < 1$.

It is now possible to test if the feature based control scheme is linearly stable regarding both focus and radial loops. It is done by using models of the focus and radial loops, the nominal controllers and the computed $\mathbf{K}_{\check{e}_{\mathrm{f}}}$ and $\mathbf{K}_{\check{e}_{\mathrm{r}}}$. The computed value in the focus case is 0.6894 and in the radial case 0.0499. It is done with the conclusion that the

linear stability criteria are fulfilled for both servo loops. I.e. as long the focus and radial servos are in the linear region these controllers are stable.

5.2 Performance of feature based control scheme

In order to inspect the performance of the algorithm it is needed to take the close loop into account. It is to determine the influence from the close loop on the approximation of the surface fault. In this regard influence will change from encounter to encounter due to the dynamics of the close loop, and since the system is linear and stable it will convergence. By inspecting Fig. 11, it can be seen that the approximation at encounter 1, $\mu = 1$.

$$\tilde{\check{\mathbf{e}}}_1^L = \mathcal{P}^{\mathrm{L}} \left(\mathbf{I} + \mathbf{S}^{\mathrm{L}} \right) \check{\mathbf{e}}_0^L, \tag{33}$$

where $\mathbf{S}^{\mathrm{L}}$ is the lifted sensitivity of the servo. At encounter $\mu = 2$ the approximation is

$$\tilde{\check{\mathbf{e}}}_2^L = \mathcal{P}^{\mathrm{L}} \left(\mathbf{I} + \mathbf{S}^{\mathrm{L}} - \mathbf{T}^{\mathrm{L}} \mathcal{P}^{\mathrm{L}} \mathbf{S}^{\mathrm{L}} \right) \check{\mathbf{e}}_1^L, \tag{34}$$

and at encounter $\mu = 3$

$$\begin{aligned} \tilde{\check{\mathbf{e}}}_3^L = & \mathcal{P}^{\mathrm{L}} \left(\mathbf{I} + \mathbf{S}^{\mathrm{L}} - \mathbf{T}^{\mathrm{L}} \mathcal{P}^{\mathrm{L}} \mathbf{S}^{\mathrm{L}} \right) \check{\mathbf{e}}_2^L \\ & + \mathbf{T}^{\mathrm{L}} \mathcal{P}^{\mathrm{L}} \mathbf{T}^{\mathrm{L}} \mathcal{P}^{\mathrm{L}} \mathbf{S}^{\mathrm{L}} \check{\mathbf{e}}_3^L. \end{aligned} \tag{35}$$

The influence from the closed loop can be determined by computing the energy of $\tilde{\check{\mathbf{e}}}_{1,2,3}$ over the energy of $\mathcal{P}^{\mathrm{L}} \check{\mathbf{e}}[n_\mu],\ \mu \in \{1, 2, 3\}$. I.e

$$\frac{\left\| \check{\mathbf{e}} - \tilde{\check{\mathbf{e}}} \right\|}{\left\| \check{\mathbf{e}} \right\|}. \tag{36}$$

These energy ratios are compute for the signals in the data set, and mean of all these ratios are following computed for focus and radial servos. The ratio for focus is 0.1134 and for radial 0.0033 for all the encounters meaning that, given this system and controller and the approximating basis and surface faults, the algorithm converge the first time it is applied. In addition it can be seen that the influence on the approximations from the controller and CD-player is small, meaning that the performance of the algorithm is almost only depending on the quality of the approximations of the surface faults, which has previous been concluded to be quit well.

6. EXPERIMENTAL RESULTS

The next step is to verify the algorithm on the experimental test setup, see Section 2.4. In this experimental work only CDs with one scratch has been used, in order to avoid book keeping of the surface faults. However, this scratch has not been included in the training set of the algorithm. The scratch has also been classified to be contained in the class of small scratches. Due to limitations in the computer power in the test setup, the algorithm was not used on both focus and radial loops at the same time. For the same reason only the method without the Kalman estimator was tested

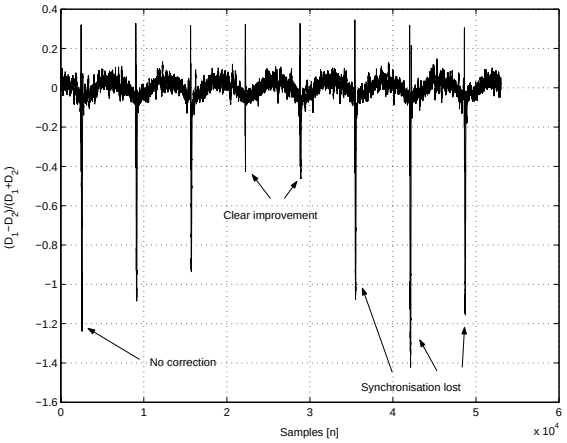

Fig. 13. A plot of the measured normalized focus difference, while the feature based correction algorithm is applied with the use of prediction of the fault location. The fault accommodation of 4th and 5th encounters of fault results in a clear improvement. Unfortunately the fault correction in the following encounters is out of synchronization. The correction results in the best case in no improvements.

with success. It has not been possible to implement the entire method due to real-time problems. However, the other optional parts of the method have previously been validated by experimental work, see (Odgaard, 2004). A scheme combining all these scheme parts is assumed to give better experimental results.

In the first experiment the fault was detected by the use of prediction of the time localization based on the location of the previous faults. A clear advantage of this approach is that the fault can be removed from the beginning of the surface fault, which should result in an almost entire removal of the scratch from the measured distances, $\mathbf{e}_{\mathrm{m}}[n]$. This approach is highly sensible to non-deterministic variations in the length of the revolutions in samples, (variations mean additional variations to the increase in the duration of one revolution with one sample for each third revolution, due to spiral shape of the information track). Analyses of the experimental data show that the variations in the duration of the revolutions vary with up to 5 samples from one revolution to the next one. Such a large variation will result in problems for the fault correction algorithm. It might cause the algorithm to result in a poorly performance. The same analyses of the experimental data also show that the length of surface faults do not change from revolution to revolution.

A couple of experiments were performed using the prediction of the fault location approach. These experiments resulted as presumed in a good fault correction when location prediction is correct. On the other hand the results were very poorly when this prediction did fail, see Fig. 13.

In Fig. 13 the potentials of the algorithm are shown at the 4th and the 5th encounter of the

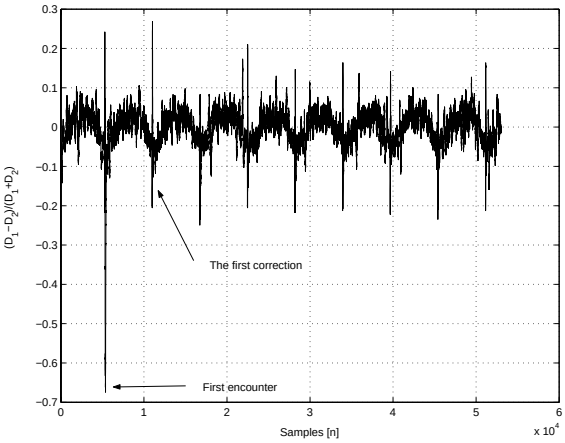

Fig. 14. A plot of the measured normalized focus difference while the correction algorithm is applied with the use of fault detection. It is clear to see that the correction results in a limitation of the influence from the fault on the measured normalized focus difference.

surface faults, where the oscillation due to the fault in $e_{\mathrm{f}}[n]$ is clearly decreased compared with the first encounter which is a correction free encounter. Unfortunately in the following encounters the location prediction fails, which result in a poorly correction of the fault, and the correction results in no improvements at all.

The prediction of the time location of the fault is used to give a region in which the fault is present. A threshold algorithm is used inside this region to locate the fault. This threshold can as a consequence be chosen lower. The fault correction is followingly applied when the fault is located and detected. It is assumed that the length of the fault is the same as at the last encounter. The length of the fault is denoted, f_{l}. The length of the correction block is 256, since $f_{\mathrm{l}} < 256$ for the entire dataset of surface faults. As long as the fault is located, the correction can be written as

$$a[n] = \begin{cases} 0 & \text{if } f_{\mathrm{d}}[n-1] = 0, \\ a[n]+1 & \text{if } f_{\mathrm{d}}[n-1] = 1. \end{cases}, \tag{37}$$

$$\grave{\mathbf{e}}[n] = \mathbf{e}_{\mathrm{m}}[n] - \begin{bmatrix} \tilde{\tilde{\mathbf{e}}}_{\mathrm{f}}[\iota] \\ \tilde{\tilde{\mathbf{e}}}_{\mathrm{r}}[\iota] \end{bmatrix}, \tag{38}$$

where

$$\iota = ((256 - l_{\mathrm{f}}) \ \mathrm{div} \ (2)) + a. \tag{39}$$

In Fig. 14 an example of this method is illustrated. The first encounter of the scratch is not corrected, but instead used to train the algorithm. In the encounters following the first one a clear improvement is achieved. It can also be seen more clear from the zoom on the 1st and 5th encounter of the fault, see Fig. 15.

Following the algorithm was tested on the radial servo loop, which is known as being more sensitive to faults than the focus servo. An example of the algorithm handling a scratch can be seen in Fig. 16. The nominal controller actually looses the radial tracking in the example in Fig. 16 which

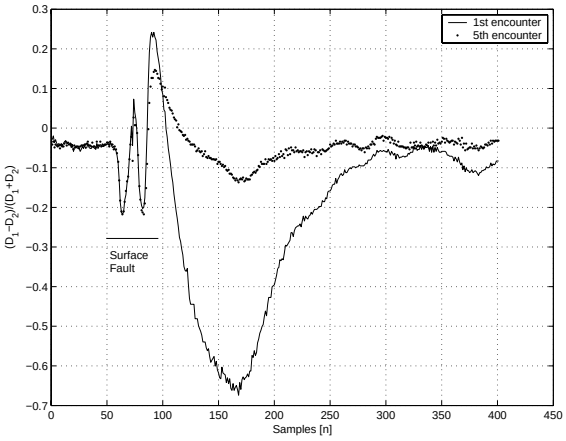

Fig. 15. A zoom on the 1st and 5th encounter of the fault shown in Fig. 14.

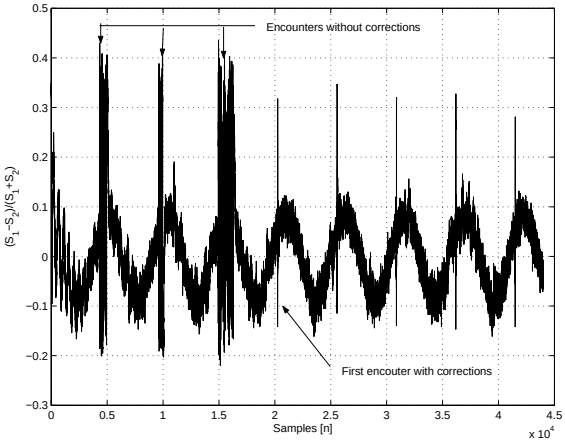

Fig. 16. A plot of the measured normalized radial difference while the fault correction algorithm is applied with the use of thresholding in a predicted interval. It is clear to see that the fault correction algorithms result in limitation of the influence from the fault on the approximated $e_{\mathrm{r}}[n]$, when the correction algorithm is applied at the 4th encounter of the fault. It can be seen that if no correction is applied the fault forces the OPU into heavy oscillations, which are avoided when the correction algorithm is used.

can be seen by the heavy oscillations. However, when the correction algorithm is applied the radial tracking is not lost. A zoom on the 2nd and 4th encounter of the fault is shown in Fig. 17.

These experimental results show that a limited version of feature based fault correction algorithm, which is proposed in this chapter, gives a clear improvement of the performance handling the surface faults, at least in the case of the tested scratches. The entire algorithm might even give better results, as simulations indicates. The feature based control scheme has not been tested on surface faults which the CD-player normally cannot play. However, it is experienced that if the controller reaction on surface faults in general is minimized, it is possible to play CDs with large surface faults. Based on this argument it can be

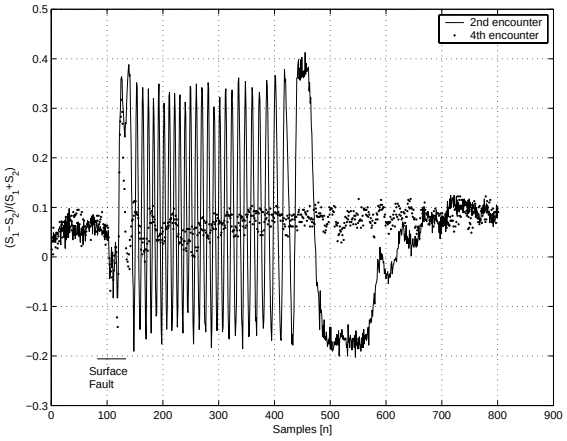

Fig. 17. A zoom on the 2nd and 4th encounter of the fault shown in Fig. 16.

concluded that the proposed feature based control scheme can improve the handling of CDs with surface faults, which cannot be handled by the nominal controllers.

7. CONCLUSION

In this paper the feature based control scheme for CD-players has been derived and verified. This scheme is essentially a fault tolerant control scheme. The fault accommodation part of the feature based control algorithm is based on removal of the influence from the surface faults. The surface faults are approximated by computing the projection of the normalized measured focus and radial differences feedback on the Karhunen-Loève bases vector approximating the surface faults. The estimated fault free distance signals are computed by subtracting the estimated surface fault from the measured distance signals. Some stability and performance issues of the feature based control algorithm are discussed, and it is proven that the scheme is linearly stable, based on a linear model of the CD-player. The scheme is verified by experimental results, in which a limited version of the feature based control scheme is used.

8. ACKNOWLEDGMENT

The authors acknowledge the Danish Technical Research Council, for support to the research program WAVES (Wavelets in Audio Visual Electronic Systems), grant no. 56-00-0143. The authors give their thanks to Department of Mathematics, Washington University in St. Louis, for hosting the first author during some of the research for this paper.

REFERENCES

Andersen, P., T. Pedersen, J. Stoustrup and E. Vidal (2001). Method for improved reading of digital data disc. International patent, no. WO 02/05271 A1.

Bouwhuis, W., J. Braat, A. Huijser, J. Pasman, G. van Rosmalen and K. Schouhamer Immink (1985). *Principles of Optical Disc Systems*. Adam Hilger Ltd.

Dötch, G.M., T. Smakman, P.M.J. Van den Hof and M. Steinbuch (1995). Adaptive repetitive control of a compact disc mechanism. In: *Proceedings of the 34th IEEE Conference on Decision and Control*. New Orleans, LA ,USA.

Draijer, W., M. Steinbuch and O.H. Bosgra (1992). Adaptive control of the radial servo system of a compact disc player. *Automatica* **28**(3), 455–462.

Fujiyama, K., M. Tomizuka and R. Katayama (1998). Digital tracking controller design for cd player using disturbance observer. In: *International Workshop on Advanced Motion Control*. Coimbra, Portugal.

Hearns, G. and M.J. Grimble (1999). Limits of performance of an optical disk drive controller. In: *Proceedings of the 1999 American Control Conference*. San Diego, CA, USA.

Heertjes, M. and F. Sperling (2003). A nonlinear dynamic filter to improve disturbance rejection in optical storages drives. In: *Proceedings of the 42nd IEEE Conference on Decision and Control*. Maui, HI, USA.

Heertjes, M. and M. Steinbuch (2004). Stability and performance of a variable gain controller with application to a dvd storage drive. *Automatica* **40**(4), 591–602.

Khargonekar, P.P., K. Poolla and A. Tannenbaum (1985). Robust control of linear time-invariant plants using periodic compensation. *IEEE Transaction on Automatic Control* **30**(11), 1088 – 1096.

Kraut, S., R.H. Andersen and J.L Krolik (2004). A generalized karhunen-loeve basis for efficient estimation of tropospheric refractivity using radar clutter. *IEEE Transaction on Signal Processing* **52**(1), 48–60.

Li, J. and T-C. Tsao (1999). Rejection of repeatable and non-repeatable disturbances for disk drive actuators. In: *Proceedings of the 1999 American Control Conference*. San Diego, CA, USA.

Mallat, S. (1999). *A wavelet tour of signal processing*. second. ed.. Academic Press.

Odgaard, Peter Fogh (2004). Feature Based Control of Compact Disc Players. PhD thesis. Department of Control Engineering, Aalborg University. ISBN:.

Odgaard, P.F. and M.V. Wickerhauser (2003*a*). Discrimination between different kind of surface defects on compact discs. Submitted for publication.

Odgaard, P.F. and M.V. Wickerhauser (2003*b*). Time localisation of surface defects on optical discs. To appear in IEEE CCA 2004.

Odgaard, P.F., J. Stoustrup, P. Andersen and H.F. Mikkelsen (2002). Extended version of: Modelling of the optical detector system in a compact disc player. www.control.aau.dk/~odgaard/papers/opmodel.pdf.

Odgaard, P.F., J. Stoustrup, P. Andersen and H.F. Mikkelsen (2003*a*). Estimation of residuals and servo signals for a compact disc player. Submitted for journal publication.

Odgaard, P.F., J. Stoustrup, P. Andersen and H.F. Mikkelsen (2003*b*). Extracting focus and radial distances, fault features from cd player sensor signals by use of a kalman estimator. In: *Proceedings of the 42nd IEEE Conference on Decision and Control*. Maui, Hawaii, USA.

Odgaard, P.F., J. Stoustrup, P. Andersen and H.F. Mikkelsen (2003*c*). Modelling of the optical detector system in a compact disc player. In: *Proceedings of the 2003 American Control Conference*. Denver, USA.

Odgaard, P.F., J. Stoustrup, P. Andersen and H.F. Mikkelsen (2004). Fault detection for compact disc players based on redundant and non-linear sensors. To appear in proceedings of American Control Conference 2004.

Odgaard, P.F., J. Stoustrup, P. Andersen, M.V. Wickerhauser and H.F. Mikkelsen (2003*d*). A simulation model of focus and radial servos in compact disc players with disc surface defects. To appear in IEEE CCA 2004.

Philips (1994). *Product specification: Digital servo processor DSIC2, TDA1301T*. Philips Semiconductors. Eindhoven, The Netherlands.

Saito, N (1998). The least statically-dependent basis and its applications. In: *Conference Record of the Thirty-Second Asilomar Conference on Signals, Systems & Computers*. Pacific Grove, CA, USA.

Stan, Sorin G. (1998). *The CD-ROM drive*. Kluwer Academic Publishers.

Steinbuch, M., G. Schoostra and O.H. Bosgra (1992). Robust control of a compact disc player. In: *Proceedings of the 31st IEEE Conference on Decision and Control*. Tucson, Arizona, USA.

Vidal, E., J. Stoustrup, P. Andersen, T.S. Pedersen and H.F. Mikkelsen (2001*a*). Open and closed loop parametric system identification in compact disk players. In: *ACC2001*. Arlington, Virginia.

Vidal, E., K.G. Hansen, R.S. Andersen, K.B. Poulsen, J. Stoustrup, P. Andersen and T.S. Pedersen (2001*b*). Linear quadratic control with fault detection in compact disk players. In: *Proceedings of the 2001 IEEE International Conference on Control Applications*. Mexico City, Mexico.

Vidal Sánchez, Enrique (2003). Robust and Fault Tolerant control of CD-players. PhD thesis. Department of Control Engineering, Aalborg University. ISBN: 87-90664-15-9.

Weerasooriya, S. and D.T. Phan (1995). Discrete-time LQG/LTR design and modeling of a disk drive actuator tracking servo system. *IEEE Transactions on Industrial Electronics* **42**(3), 240–247.

Wickerhauser, Mladen Victor (1994*a*). Large-rank approximate principal component analysis with wavelets for signal feature discrimination and the inversion of complicated maps. *Journal of Chemical Information and Computer Science* **34**(5), 1036–1046.

Wickerhauser, M.V. (1994*b*). *Adapted Wavelet Analysis from Theory to Software*. 1st ed.. A K Peters, Ltd.

Wisniewski, R. and J. Stoustrup (2001). Generalized H_2 control synthesis for periodic systems. In: *American Control Conference 2001*. Arlington, Virginia, USA.

Wook Heo, J. and J. Chung (2002). Vibration and noise reduction of an optical disk drive by using a vibration absorber. *IEEE Transactions on Consumer Electronics* **48**(4), 874 – 878.

Yao, L., A.-M. Wang and Y.-F. Cheng (2001). Track seeking hybrid fuzzy controller for the compact disc player. In: *The 10th IEEE International Conference on Fuzzy Systems*. Melbourne, Australia.

Yen, J-Y., C-S. Lin and Y-Y. Li, C-H. Chen (1992). Servo controller design for an optical disk drive using fuzzy control algorithm. In: *IEEE International Conference on Fuzzy Systems*. San Diego, CA, USA.